Hawaii Rainfall Anomalies and El Niño*

PAO-SHIN CHU

Department of Meteorology, School of Ocean and Earth Science and Technology, University of Hawaii, Honolulu, Hawaii

7 July 1994 and 20 December 1994

ABSTRACT

An analysis of composite, seasonal rainfall anomalies in Hawaii shows that deficient rainfall tends to occur frequently in winter and spring of the year following an El Niño. The reliability of the El Niño composite has been tested using a Monte Carlo simulation technique. Upper-air circulation patterns during the recent three El Niño events are discussed in relation to drought winters in Hawaii. The more eastward elongated subtropical jet stream in the North Pacific and the thermally induced local Hadley circulation in the central North Pacific, characteristics of El Niño winters, are unfavorable for rainfall in Hawaii.

1. Introduction

Many tropical Pacific islands are experiencing a rapid population increase that places an increasing demand on water for drinking, food production, and other needs. If the current trend continues, many islands may be faced with a shortage of freshwater in the near future. Further compounding this problem is the great variability of interannual rainfall in this region. This uncertainty in rainfall from year to year, together with the increasing demand for water, requires a better understanding of the relationship between rainfall and short-term climate variability.

Drought in Hawaii usually occurs after an El Niño event (Meisner 1976; Horel and Wallace 1981; Lyons 1982; Ropelewski and Halpert 1987; Chu 1989; Cayan and Peterson 1989). Based on three stations in Hawaii, Ropelewski and Halpert (1987) composited the monthly rainfall index during an El Niño cycle. Ropelewski and Halpert (hereafter referred to as RH) showed that October of the El Niño year to May of the year following an El Niño tends to be dry. The current paper further addresses the RH study by utilizing more rainfall station data in Hawaii. A more comprehensive spatial coverage of rain gauge network is needed to account for the well-known marked rainfall variations on the windward and leeward sides of the island (Giambelluca et al. 1986). The reliability of the El Niño composite rainfall, which is not addressed by RH, will be assessed by Monte Carlo sampling techniques. To shed light on the mechanisms of rainfall anomalies in Hawaii, prominent circulation patterns in the central North Pacific during the recent three El Niño events will be discussed.

2. Data and data processing

The location of long-term rainfall stations used in this study is shown in Fig. 1 and listed in Table 1. As in Meisner (1976) and Chu (1989), nine stations from each of three islands (Kauai, Oahu, and Hawaii) are selected. These 27 stations are representative of the spatial variability of rainfall with regard to the direction of the prevailing northeast trade winds and to varying elevation levels. Because some of the stations discontinued for a variety of reasons, more recent records from adjacent stations in the same climatic regime are used (Table 1). For example, on Kauai, rainfall records from Iliilula Intake are replaced by North Wailua Ditch since 1987. As a result, a majority of stations have records updated to 1992. A normalization technique is applied to each individual station, and a regional index is then calculated as the arithmetic average of all station indices from three islands. The base period is 1905–1992.

Upper-air data of wind velocity and geopotential height on 5° latitude–longitude grids at 850 and 200 hPa are obtained from the European Centre for Medium-Range Weather Forecasts. The outgoing longwave radiation (OLR) records over the tropical belts (22.5°N to 22.5°S) from NOAA's scanning or Advanced Very High Resolution Radiometer mounted on polar-orbiting satellites are available at 2.5° latitude–longitude resolution.

* SOEST Contribution Number 3852.

Corresponding author address: Dr. Pao-Shin Chu, Department of Meteorology, University of Hawaii at Manoa, 2525 Correa Road, HIG 331, Honolulu, HI 96822.

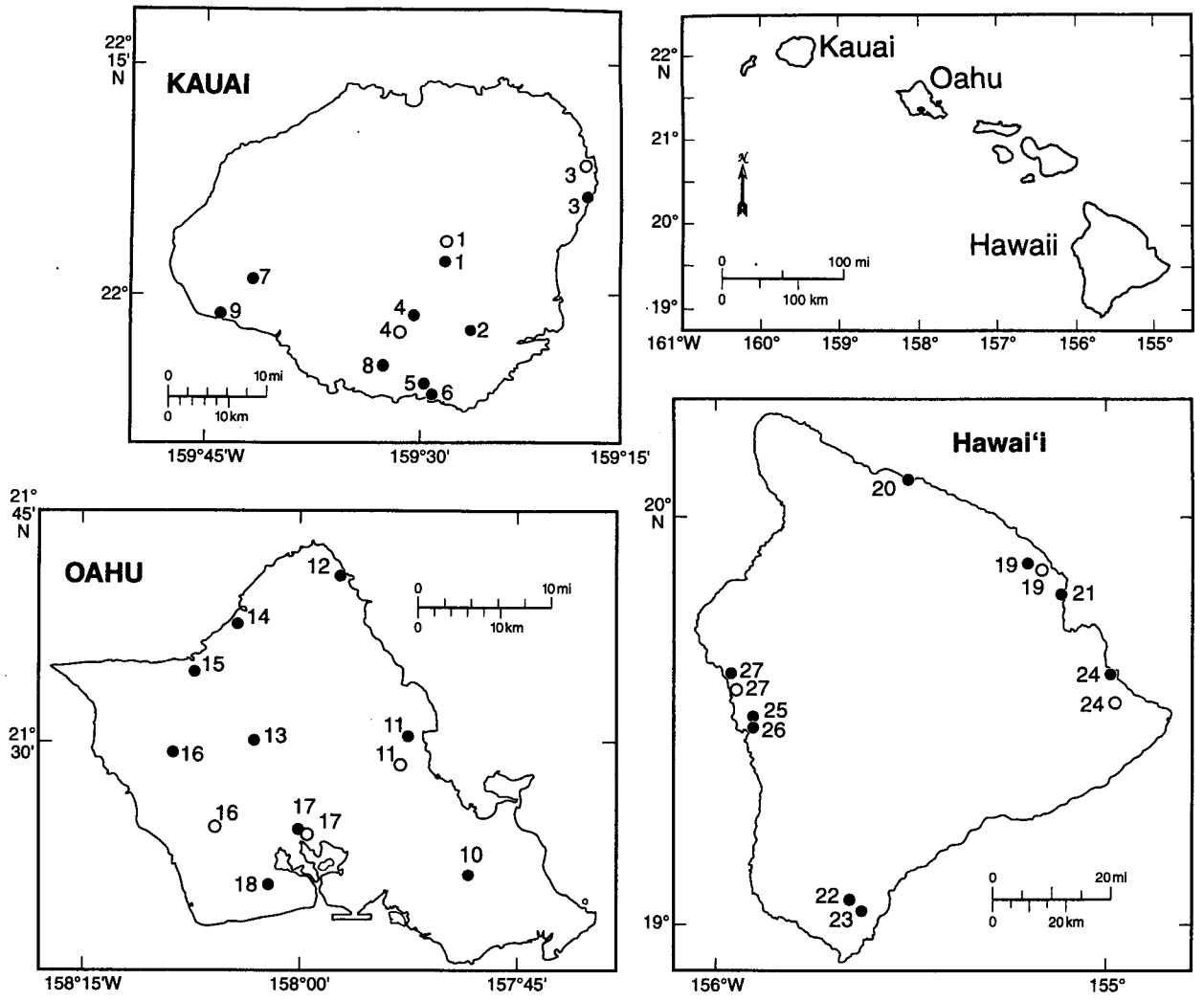

FIG. 1. Map of the major Hawaiian Islands and the locations of rainfall stations used in this study. Station numbers are the same as listed in Table 1. An open circle indicates a new station.

3. Rainfall fluctuations

a. Composite rainfall

Figure 2 shows a time series of composite seasonal rainfall anomalies for Hawaii during the 20 El Niño events. The year in which El Niño has occurred is denoted as (0); the year immediately following (0) is (+1). The 20 (0) and (+1) pairs comprise 1905–1906, 1911–1912, 1914–1915, 1918–1919, 1923–1924, 1925–1926, 1930–1931, 1932–1933, 1939–1940, 1941–1942, 1951–1952, 1953–1954, 1957–1958, 1965–1966, 1969–1970, 1972–1973, 1976–1977, 1982–1983, 1986–1987, and 1991–1992 (cf. RH). Winter is defined from December of the preceding year to February of the following year. For example, winter of 1987 runs from December 1986 through February 1987.

In Fig. 2, rainfall anomalies tend to be small positive from spring to fall (0). Deficient rainfall persists from winter to fall of the following year (+1), with a large negative anomaly occurring in winter and spring. This result suggests that El Niño–related drought in Hawaii is persistent, lasting for about six months. Particularly noteworthy is the high frequency of low rainfall occurrence in winter (+1). In this limited sample, the chance is 90% that below average rainfall would occur in the winter of (+1). Because the bulk of annual rainfall in Hawaii comes in winter and spring, the large deficit of rainfall and high probability of low rainfall in these two seasons are a robust indicator of the overall shortage in the water supply for the year immediately following an El Niño event. After spring (+1), there is an almost equal chance for rainfall anomalies to be either positive or negative.

TABLE 1. List of rainfall stations in this study. Stations on each island are arranged so that the first three stations are windward, the next three are neutral, and the last three are leeward. For each side of the island, the station is arranged from high to low elevation. Solidus denotes replacement station follows. Asterisk denotes new stations.

Station	Code number	Lat (N)/long (W)	Elevation (m)	Record length
Kauai				
1. Iliilula	1050.00	22 02 34/159 28 18	326.2	1935–1986
Intake/				
North Wailua	1051.00	22 03 57/159 28 12	338.4	1987–1992
Ditch*				
2. Koloa Mauka	994.00	21 57 50/159 26 36	195.1	1905–1992
3. Kealia/	1112.00	22 06 10/159 18 30	3.0	1905–1986
Anahola*	1114.00	22 08 15/159 18 24	54.9	1987–1992
4. Wahiawa Mt./	990.00	21 58 30/159 30 35	655.4	1905–1972
Alexander Reservoir*	983.00	21 57 34/159 31 43	423.6	1973–1992
5. East Lawai	934.00	21 54 30/159 29 48	134.1	1905–1992
6. Kukuiula	935.00	21 53 30/159 29 30	32.0	1905–1992
7. Puehu Ridge	1040.00	22 01 07/159 41 42	506.1	1940–1992
8. Brydeswood Station	985.00	21 55 42/159 32 12	219.5	1910–1992
9. Waiawa	943.00	21 58 50/159 43 58	3.0	1905–1992
Oahu				
10. Nuuanu Res.	783.00	21 21 21/157 48 37	320.1	1905–1992
11. Waikane/	885.00	21 30 12/157 53 24	243.9	1917–1982
Waiahole*	837.00	21 28 24/157 52 58	227.1	1983–1992
12. Kahuku	912.00	21 40 48/157 57 12	7.6	1905–1992
13. Wahiawa Dam	863.00	21 30 00/158 03 08	260.6	1905–1992
14. Waimea	892.00	21 37 43/158 04 03	128.0	1917–1992
15. Waialua	847.00	21 34 36/158 07 24	4.5	1905–1992
16. Waianae Mauka/	803.00	21 29 25/158 08 04	480.1	1905–1973
Hokuloa*	725.20	21 24 36/158 05 48	594.7	1974–1992
17. Aiea Field/	761.00	21 24 30/157 56 36	138.7	1908–1969
Aiea*	764.50	21 24 26/157 54 35	213.4	1970–1983
18. Ewa Mill	741.00	21 20 38/158 02 12	22.8	1905–1992
Hawaii				
19. Hakalau Mauka/	135.00	19 53 12/155 10 06	350.6	1906–1978
Honomu Mauka*	138.00	19 51 06/155 08 48	382.8	1979–1992
20. Paauhau	217.00	20 05 12/155 26 24	121.9	1905–1992
21. Papaiku Makai	144.10	19 47 12/155 04 42	60.9	1905–1992
22. Kiolakaa	6.00	19 04 24/155 38 18	586.8	1929–1987
23. Naalehu	14.00	19 03 48/155 35 24	205.7	1905–1992
24. Kapolo/	93.00	19 30 36/154 50 36	33.5	1905–1959
Hayhalalekai*	67.50	19 28 30/154 50 06	4.6	1960–1980
25. Kaawaloa	29.00	19 29 42/155 55 12	408.5	1942–1992
26. Napoopoo	28.00	19 28 18/155 54 30	121.9	1940–1992
27. Holualoa Beach/	68.00	19 36 30/155 58 47	3.0	1919–1978
Kainaliu Beach*	73.12	19 31 54/155 57 24	5.2	1979–1989

b. Monte Carlo simulation

As mentioned previously, the frequency of low rainfall occurrence in some seasons during the El Niño composite is very high. A natural question asked is whether other randomly selected composites could have produced the same kind of statistic as the El Niño composite. A null hypothesis is formed such that the frequency of occurrence of negative rainfall anomalies during the El Niño composite (20 events) is equivalent to a sample randomly formed from the rainfall record.

The 88-yr (1905–1992) record is scrambled into a group of 20 yr using a random number generator. This procedure is then repeated in a very large number of trials. According to Noreen (1989), the significance level of the test is $(n + 1)/(N + 1)$, where n is the number of simulated samples for which the values of the test statistic (frequency of occurrence of negative rainfall anomalies) is equivalent to the test statistic for the El Niño composite, and N is the number of simulated random samples. In this study, $N = 999$.

Table 2 lists the significance level of the simulation through an El Niño cycle. The most striking case is the winter (+1); namely, the probability of obtaining a test statistic comparable to that observed during an El Niño cycle in the winter (+1) is extremely small (0.1%) in a random size of 999. This suggests that deficient rainfall observed during winter (+1) was very unlikely to have occurred by random chance. For spring (+1), the probability of getting a value from the random sample comparable to the corresponding El Niño sta-

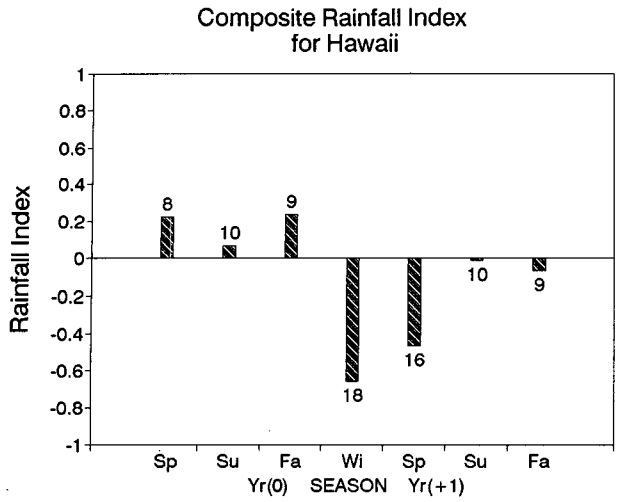

FIG. 2. Time series of composite seasonal rainfall index in Hawaii during an El Niño cycle. Normalized value is used. For a particular season, the number of total seasons with a negative rainfall index during 20 El Niño events is indicated in the diagram.

tistics is low, about 1%. These results support the earlier finding presented in Fig. 2.

4. Upper-air circulation patterns

In this section, upper-air circulation patterns during the recent three El Niño winters are presented. The distribution of geopotential height at 850 hPa in the central North Pacific during the winter of 1983 is shown in Fig. 3a. Clearly, Hawaii is located in a region of an elongated and extensive subtropical ridge where sinking motion prevails. For winter 1987 (Fig. 3b), the subtropical ridge is divided into two cells and Hawaii is on the eastern flank of the western cell in an area of divergence associated with equatorward motions and anticyclonic flows. The geopotential height pattern during winter of 1992 is reminiscent of that during winter of 1983 (Figs. 3a,c) in that Hawaii is embedded within an extensive subtropical ridge system.

Height anomalies at 200 hPa during winter of 1983 are shown in Fig. 3d. Large negative anomalies are found in the midlatitude ocean, with the largest value in the Gulf of Alaska. Positive height anomalies prevail in the lower latitudes and Hawaii is located near a large positive anomaly center. Based on the data up to 1980, Taylor (1984) suggested that positive anomalies at 200 hPa over Hawaii during winter are manifestations of an intensification and eastward displacement of the western Pacific subtropical ridge. Combining features from lower and upper troposphere during winter 1983 (Figs. 3a,d), one notes that the strengthening of the subtropical ridge extends throughout the entire troposphere. The meridional contrast of geopotential height anomaly presented in Fig. 3d favors the buildup of anomaly thermal winds in the eastern North Pacific, which in turn strengthen the westerly jet. During winter of 1987 (Fig. 3e), the midlatitude central North Pacific is characterized by negative height anomalies, and the lower latitudes are characterized by small positive anomalies, a pattern similar to that in Fig. 3d, albeit with a weaker magnitude. For winter 1992 (Fig. 3f), negative height anomalies and positive anomalies still dominate a large portion of the midlatitude and subtropical central Pacific, respectively.

Figure 4a presents the 200-hPa winter mean winds. The subtropical jet stream core at 200 hPa, defined as a region where wind speed exceeds 40 m s^{-1}, extends from the western Pacific to about 155°W. During winter of 1983 (Fig. 4b), the jet core extends well eastward to about 130°W, a feature consistent with the distribution of strong height anomalies demonstrated in Fig. 3d. Hawaii is located near the right exit region of the jet core (Fig. 4b) in an area of upper-level convergence that is conducive to midtropospheric subsidence and lower-tropospheric divergence. For winter 1987 (Fig. 4c), the leading edge of the jet core shows more eastward displacement relative to climatology (Fig. 4a). As a result, Hawaii is located closer to the right exit region of the jet. During winter 1992 (Fig. 4d), the subtropical jet is again elongated eastward. Arkin (1982) composited 200-hPa winds during the three El Niño winters (1969–1970, 1972–1973, and 1976–1977), which are not included in the current analysis. His results also showed that the North Pacific jet extended farther eastward following the onset of El Niño.

An additional insight into the relationship between winter rainfall in Hawaii and large-scale circulation can be gained by examining changes in OLR at the height of El Niño. In the Tropics, an inverse relationship generally holds between OLR and convection. Thus, anomalously low (high) OLR values correspond to enhanced (reduced) convection. OLR also has been used directly to estimate tropical precipitation (e.g., Motell and Weare 1987).

Figure 5 shows the spatial distribution of OLR anomalies during winters of 1983, 1987, and 1992. A large area of strong negative anomalies, indicative of enhanced convection and ascending motion, is found in the equatorial central Pacific for all three El Niño winters. The tremendous release of latent heat in convective precipitation not only drives tropical atmospheric circulation over the Pacific Ocean but also has

TABLE 2. The probability of falsely rejecting the null hypothesis in $N = 999$ Monte Carlo trials through an El Niño cycle. The (0) denotes the El Niño year and (+1) denotes the year immediately following (0). The numbers in boldface exceed the conventional 5% significance level.

	Winter	Spring	Summer	Fall
(0)	0.080	0.067	0.188	0.191
(+1)	**0.001**	**0.014**	0.204	0.189

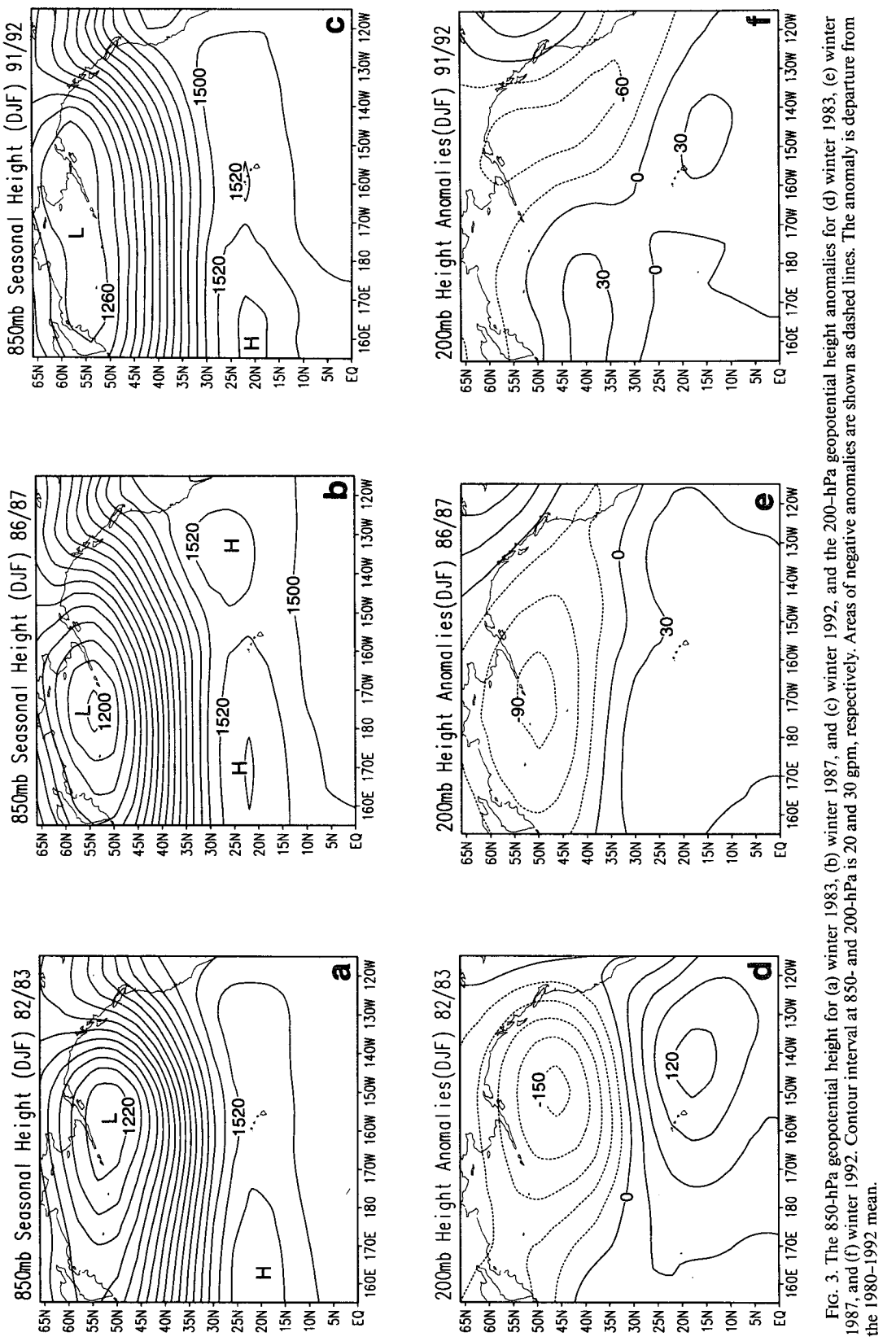

FIG. 3. The 850-hPa geopotential height for (a) winter 1983, (b) winter 1987, and (c) winter 1992, and the 200-hPa geopotential height anomalies for (d) winter 1983, (e) winter 1987, and (f) winter 1992. Contour interval at 850- and 200-hPa is 20 and 30 gpm, respectively. Areas of negative anomalies are shown as dashed lines. The anomaly is departure from the 1980–1992 mean.

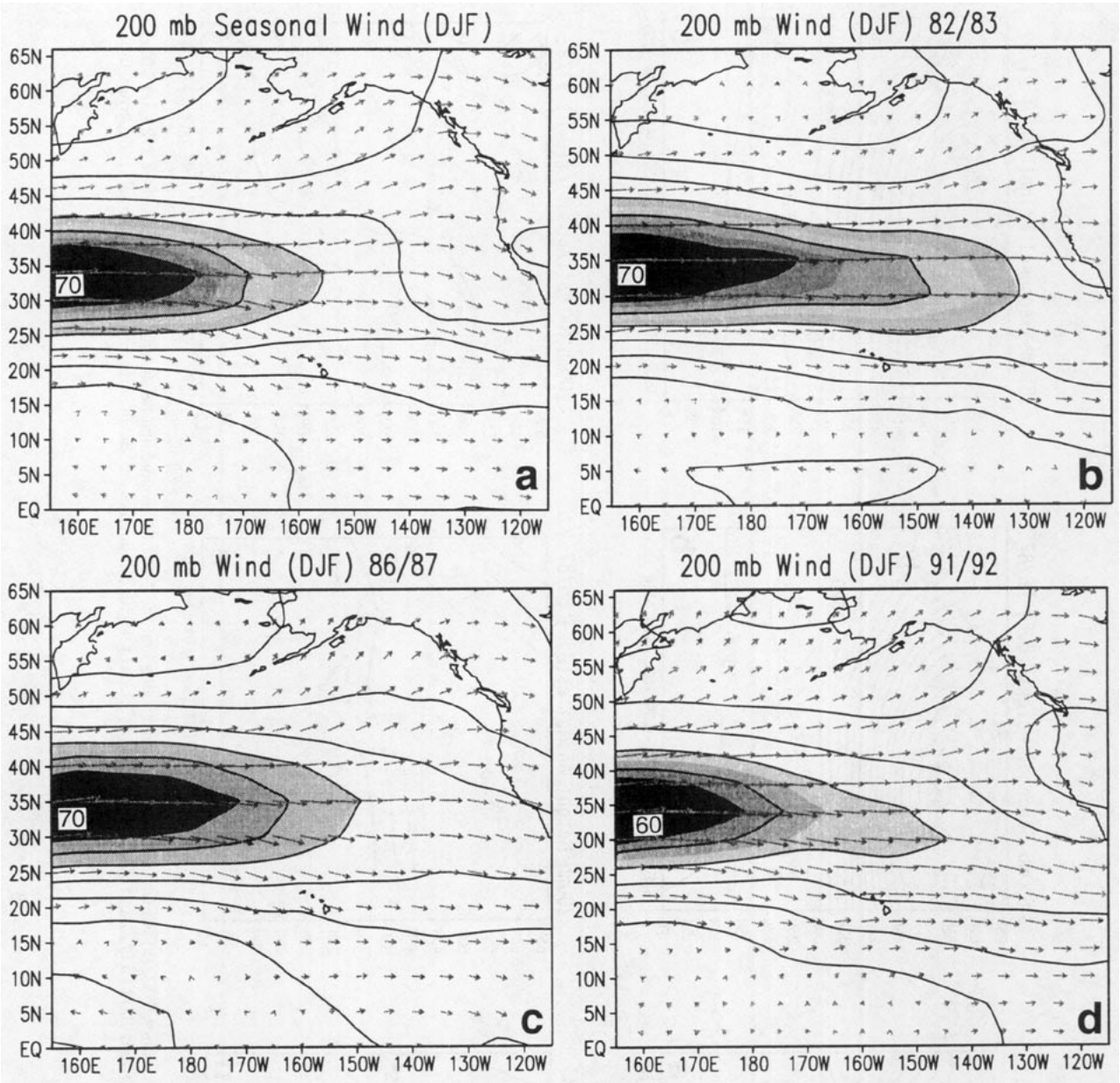

FIG. 4. The 200-hPa wind field for (a) the 1980–1992 mean, (b) winter 1983, (c) winter 1987, and (d) winter 1992. Isotach interval is 10 m s^{-1}. Area with wind speed greater than 40 m s^{-1} is shaded.

profound effects on the global teleconnection patterns (e.g., Rasmusson 1991). Small positive OLR anomalies, indicative of reduced convection and enhanced sinking motions, prevail in the subtropical North Pacific.

5. Summary and discussion

The results demonstrated here suggest that the occurrence of deficient rainfall in Hawaii in the winter and spring of the year immediately subsequent to El Niño is high. Considerations about the physical causes of these relationships follow. At the height of El Niño events, warm pools of sea water and the attendant convection shift eastward to the equatorial central Pacific. The enhanced tropical convection results in a strong ascending motion, which leads to strong Hadley-type circulation in the central North Pacific. Because Hawaii is located in the sinking portion of the Hadley cell, synoptic systems such as Kona storms and midlatitude frontal rainband that usually produce winter rainfall in the islands have become unfavorable (Chu et al. 1993; Lyons 1982), and drought occurs.

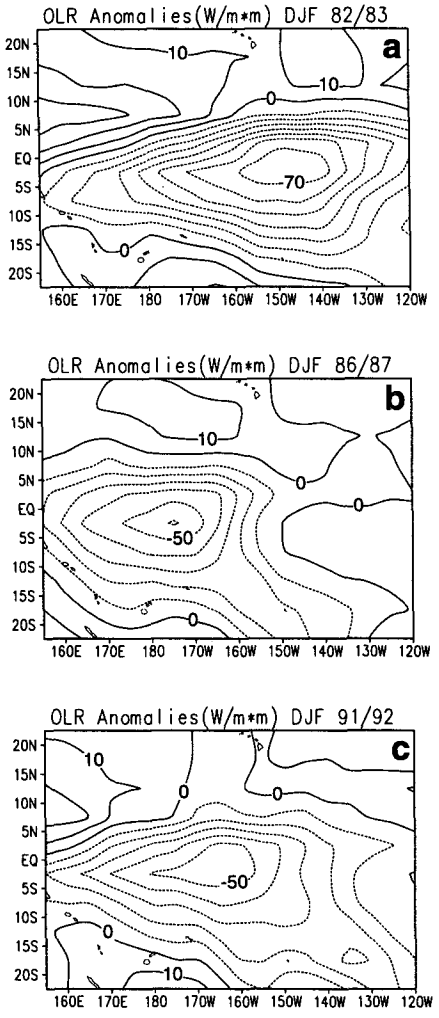

FIG. 5. The OLR anomaly for (a) winter 1983, (b) winter 1987, and (c) winter 1992. Areas of negative anomalies are shown as dashed lines. Contour interval is 10 W m^{-1}. The anomaly is departure from the 1980–1992 mean.

In addition, the strong equatorial heating associated with El Niño gives rise to positive height anomalies over the central subtropical Pacific and negative height anomalies over the midlatitudes in the upper troposphere (Fig. 3). As a result, the subtropical jet stream in the North Pacific is stronger and extends farther eastward or equatorward than average (Fig. 4). Hawaii is then located under the right exit region of the jet, which favors divergence at lower troposphere. Therefore, the anomalous displacement of the subtropical jet and the development of the local Hadley circulation in the central North Pacific are two important general circulation features that inhibit wintertime rainfall production in Hawaii.

Many other tropical Pacific islands (e.g., Guam, Fiji) have similar problems as Hawaii, namely, increasing demand for freshwater and large, natural variability in rainfall from year to year. It is hoped that the method demonstrated here would also be of value to other tropical Pacific islands in confirming the El Niño-related rainfall anomalies. If this relationship is rigorous, as is the case in Hawaii, such information would be vital to various governments in making long-range water resources planning and management.

Acknowledgments. This study was funded by the Board of Water Supply, City and County of Honolulu, Department of Land and Natural Resources, State of Hawaii, and the U.S. Geological Survey through the Water Resources Research Center, University of Hawaii. J. Wang assisted with the data processing. The author is indebted to Prof. S. Hastenrath for carefully reading the draft of the paper and to N. Nicholls and an anonymous reviewer for suggestions that improved the manuscript.

REFERENCES

Arkin, P. A., 1982: The relationship between interannual variability in the 200 mb tropical wind field and the Southern Oscillation. *Mon. Wea. Rev.*, **110,** 1393–1404.

Cayan, D. R., and D. H. Peterson, 1989: The influence of North Pacific atmospheric circulation on streamflow in the west. *Aspects of Climatic Variability in the Pacific and the Western Americas, Geophys. Monogr.*, No. 55, Amer. Geophys. Union, 375–397.

Chu, P.-S., 1989: Hawaiian drought and the Southern Oscillation. *Int. J. Climatol.*, **9,** 619–631.

——, A. J. Nash, and F. Porter, 1993: Diagnostic studies of two contrasting rainfall episodes in Hawaii: Dry 1981 and wet 1982. *J. Climate,* **6,** 1457–1462.

Giambelluca, T. S., M. A. Nullet, and T. A. Schroeder, 1986: Rainfall Atlas of Hawaii. Department of Land and Natural Resources, Report R76, State of Hawaii, Honolulu, HI, 267 pp.

Horel, J. D., and J. M. Wallace, 1981: Planetary scale atmospheric phenomena associated with the Southern Oscillation. *Mon. Wea. Rev.*, **109,** 813–829.

Lyons, S. W., 1982: Empirical orthogonal function analysis of Hawaiian rainfall. *J. Appl. Meteor.*, **21,** 1713–1729.

Meisner, B. N., 1976: A study of Hawaiian and Line Islands rainfall. Dept. of Meteorology, University of Hawaii, UHMET-76-04, 83 pp.

Motell, C. E., and B. C. Weare, 1987: Estimating tropical Pacific rainfall using digital satellite data. *J. Climate Appl. Meteor.*, **26,** 1436–1446.

Noreen, E. W., 1989: *Computer Intensive Methods for Testing Hypotheses.* Wiley and Sons, 229 pp.

Rasmusson, E. M., 1991: Observational aspects of ENSO cycle teleconnections. *Teleconnections Linking Worldwide Climate Anomalies,* M. Glantz, R. W. Katz, and N. Nicholls, Eds., Cambridge University Press, 309–343.

Ropelewski, C. F., and M. S. Halpert, 1987: Global and regional scale precipitation patterns associated with the El Niño/Southern Oscillation. *Mon. Wea. Rev.*, **115,** 1606–1626.

Taylor, G. E., 1984: Hawaiian winter rainfall and its relation to the Southern Oscillation. *Mon. Wea. Rev.*, **112,** 1613–1619.